# Supplementary information for

# Structural and Biochemical Characterization of a Dye-Decolorizing Peroxidase from *Dictyostelium discoideum*

**Amrita Rai [1,2], Johann P. Klare [3], Patrick Y. A. Reinke [1,4,5], Felix Englmaier [6,7], Jörg Fohrer [7,8], Roman Fedorov [4], Manuel H. Taft [1], Igor Chizhov [1,4], Ute Curth [1,4], Oliver Plettenburg [6,7] and Dietmar J. Manstein [1,4,9,*]**

1 Institute for Biophysical Chemistry, Hannover Medical School, Fritz Hartmann Centre for Medical Research Carl Neuberg Str. 1, D-30625 Hannover, Germany; Amrita.Rai@mpi-dortmund.mpg.de (A.R.); patrick.reinke@desy.de (P.Y.A.R.); Taft.Manuel@mh-hannover.de (M.H.T.); chizhov.igor@mh-hannover.de (I.C.); curth.ute@mh-hannover.de (U.C.)
2 Department of Structural Biochemistry, Max Planck Institute of Molecular Physiology, D-44227 Dortmund, Germany
3 Department of Physics, University of Osnabrueck, Barbarastrasse 7, D-49076 Osnabrück, Germany; jklare@uni-osnabrueck.de
4 Division for Structural Biochemistry, Hannover Medical School, Carl Neuberg Str. 1, D-30625 Hannover, Germany; Fedorov.Roman@mh-hannover.de
5 Center for Free-Electron Laser Science, German Electron Synchrotron (DESY), Notkestr. 85, D-22607 Hamburg, Germany
6 Institute of Medicinal Chemistry, Helmholtz Zentrum München (GmbH), German Research Center for Environmental Health, Ingolstädter Landstraße 1, D-85764 Neuherberg, Germany; felix.englmaier@helmholtz-muenchen.de (F.E.); oliver.plettenburg@oci.uni-hannover.de (O.P.)
7 Center of Biomolecular Drug Research (BMWZ), Institute of Organic Chemistry, Leibniz University Hannover, Schneiderberg 1b, D-30167 Hannover, Germany; joerg.fohrer@tu-darmstadt.de
8 Department of Chemistry, Clemens-Schöpf-Institute of Organic Chemistry and Biochemistry, Darmstadt Technical University, Alarich-Weiss-Strasse 4, D-64287 Darmstadt, Germany
9 Department of Chemistry, Clemens-Schöpf-Institute of Organic Chemistry and Biochemistry, Darmstadt Technical University, D-30625 Hannover, Germany
* Correspondence: Manstein.Dietmar@MH-Hannover.de; Tel.: +49-511-5323700

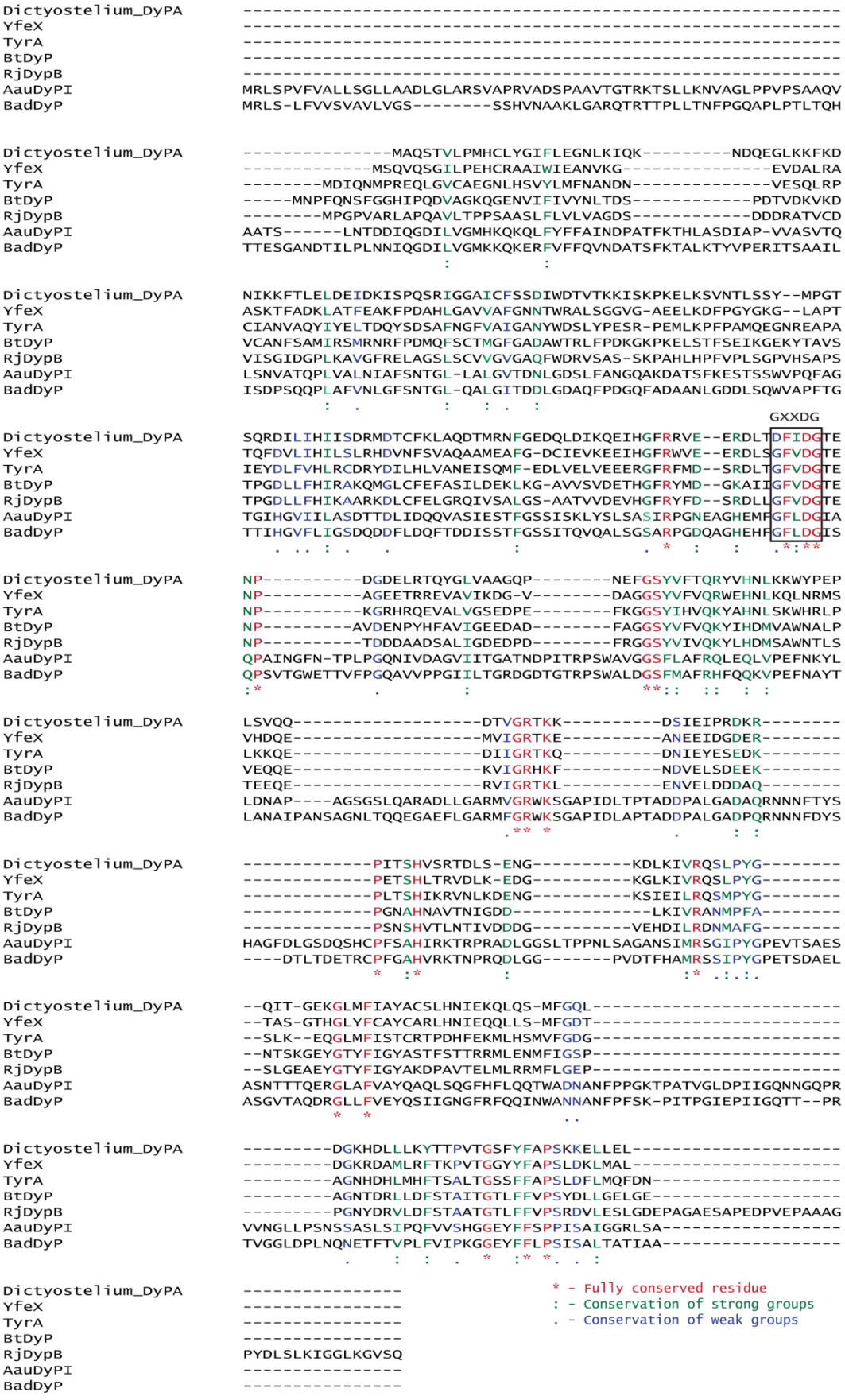


**Figure S1:** Sequence alignment of *Dictyostelium* DyPA with different bacterial and fungal DyPs. The conserved G/DXXDG motif is shown in a black box. *Dictyostelium discoideum* DyPA (UniProt ID: Q556V8), *Escherichia coli* (strain K12) YfeX (UniProt ID: P76536), *Shewanella oneidensis* (strain MR-1) TyrA (UniProt ID: Q8EIU4), *Bacteroides*

*thetaiotaomicron* VPI-5482 *Bt*DyP (UniProt ID: Q8A8E8), *Rhodococcus jostii* RHA1 *Rj*DyPB (UniProt ID: Q0SE24), *Auricularia auricula-judae Aau*DyPI (UniProt ID: I2DBY1), *Bjerkandera adusta Bad*DyP (UniProt ID: Q8WZK8)

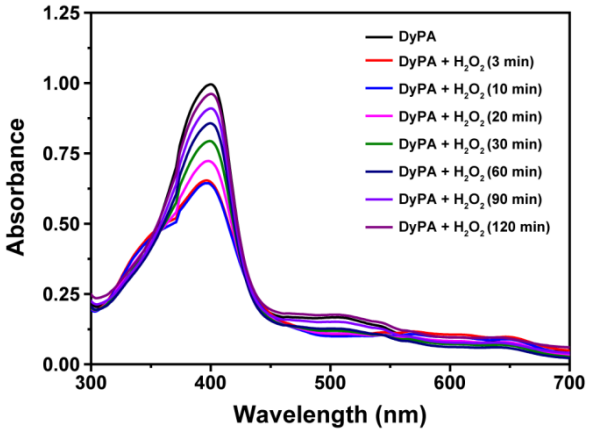


**Figure S2:** UV-visible absorption spectra of *Dictyostelium* DyPA in the presence of $H_2O_2$. Spectra of 10 μM *Dictyostelium* DyPA in the absence (black) or in the presence (red to magenta) of 10 μM $H_2O_2$ at different time points. Measurements performed in buffer containing 50 mM Tris pH 8.0, 150 mM NaCl at 23°C.

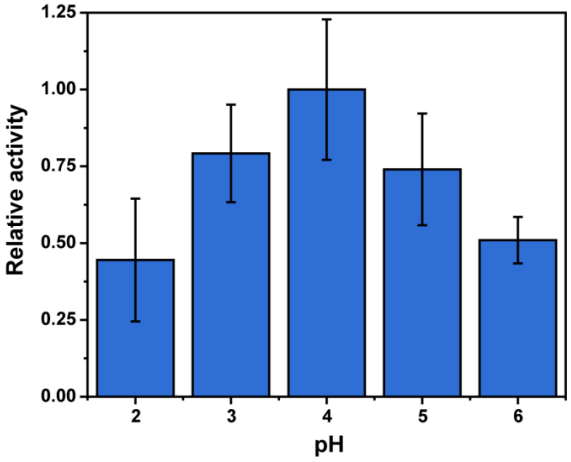


**Figure S3:** Optimum pH for the oxidation of veratryl alcohol by *Dictyostelium* DyPA. Assays were performed in 100 μl of 50 mM sodium acetate (pH 2.0 – 6.0) and 150 mM NaCl at 25 °C, containing 10 mM VA and 4 μM *Dictyostelium* DyPA. Reactions were initiated by the addition of 1 mM $H_2O_2$ and monitored at 310 nm (VA $\varepsilon_{310}$= 9.3 $mM^{-1}$ $cm^{-1}$). Data are average values of 3–6 independent measurements; bars represent the standard deviation.

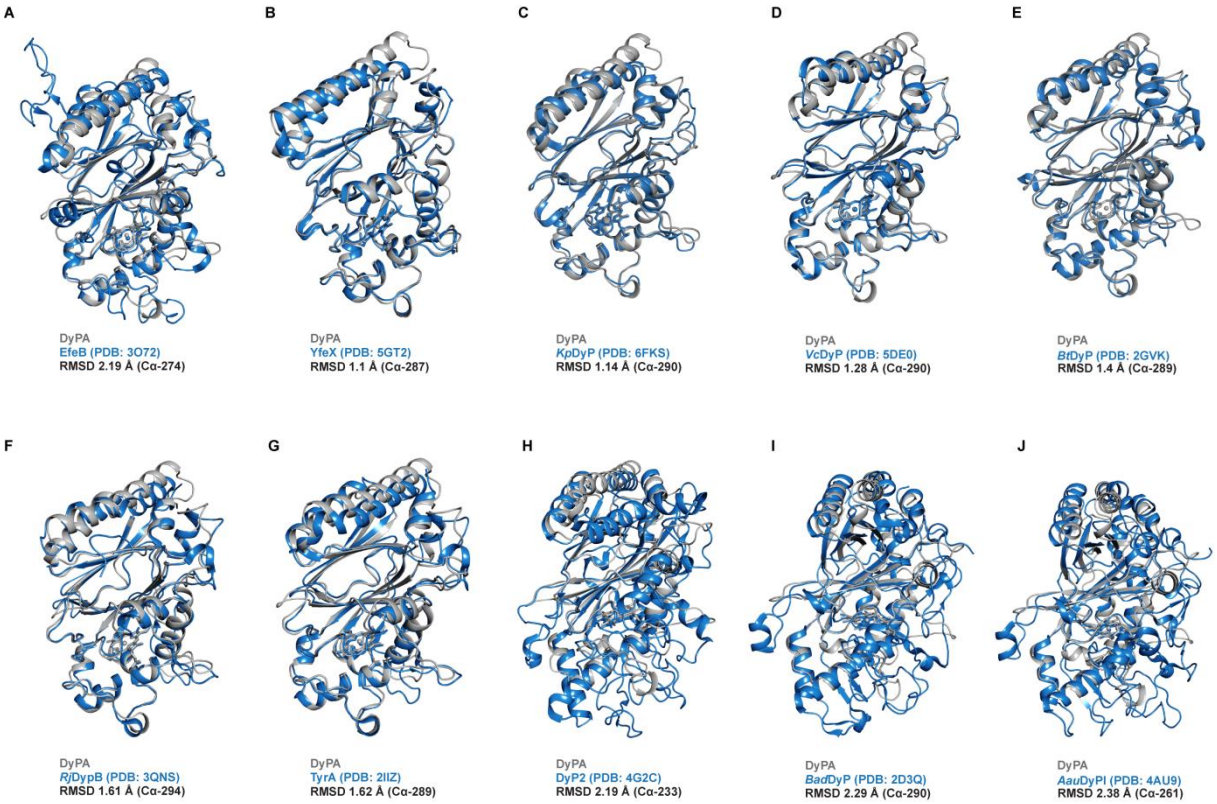


**Figure S4**. Structural comparison of *Dictyostelium* DyPA with related bacterial and fungal dye decolorizing peroxidases. Structural alignment of *Dictyostelium* DyPA (grey) with **(A)** *Escherichia coli* O157 EfeB (blue; class A). **(B)** *Escherichia coli O157* YfeX (blue; class B). **(C)** *Klebsiella pneumoniae Kp*DyP (blue; class B). **(D)** *Vibrio cholerae Vc*DyP (blue; class B). **(E)** *Bacteroides thetaiotaomicron* VPI-5482 *Bt*DyP (blue; class B). **(F)** *Rhodococcus jostii RHA1 Rj*DypB (blue; class B). **(G)** *Shewanella oneidensis* TyrA (blue; class B). **(H)** *Amycolatopsis sp.* 75iv2 DyP2 (blue; class C). **(I)** *Bjerkandera adust*a *Bad*DyP (blue; class D). **(J)** *Auricularia auricula-judae Aau*DyPI (blue; class D).

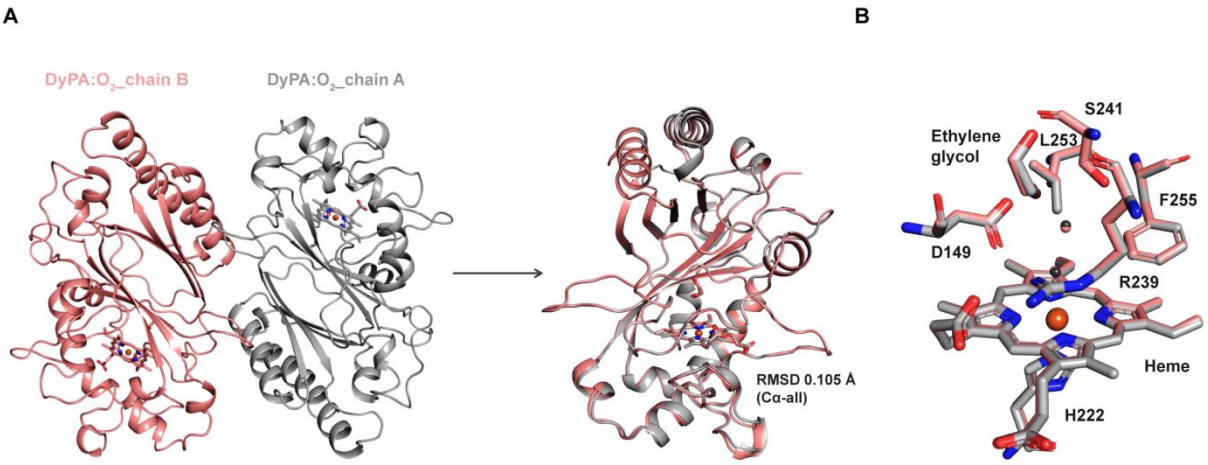


**Figure S5:** Structure of the *Dictyostelium* DyPA:$O_2$ complex. **(A)** The asymmetric unit contains two nearly identical copies of DyPA, as shown by the overlay of both structural models. **(B)** Heme microenvironment of the *Dictyostelium* DyPA:$O_2$ complex. Grey/salmon pink spheres show the position of the oxygen atoms in the *Dictyostelium* DyPA:$O_2$ complex structure.

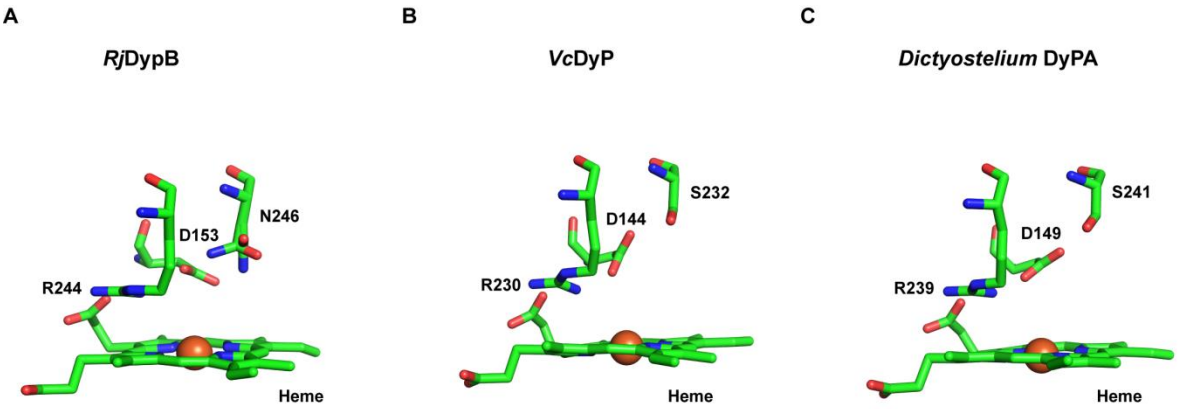


**Figure S6**. Heme microenvironment. **(A)** *Rj*DypB (PDB: 3QNS), **(B)** *Vc*DyP (PDB: 5DE0) and **(C)** *Dictyostelium* DyPA.

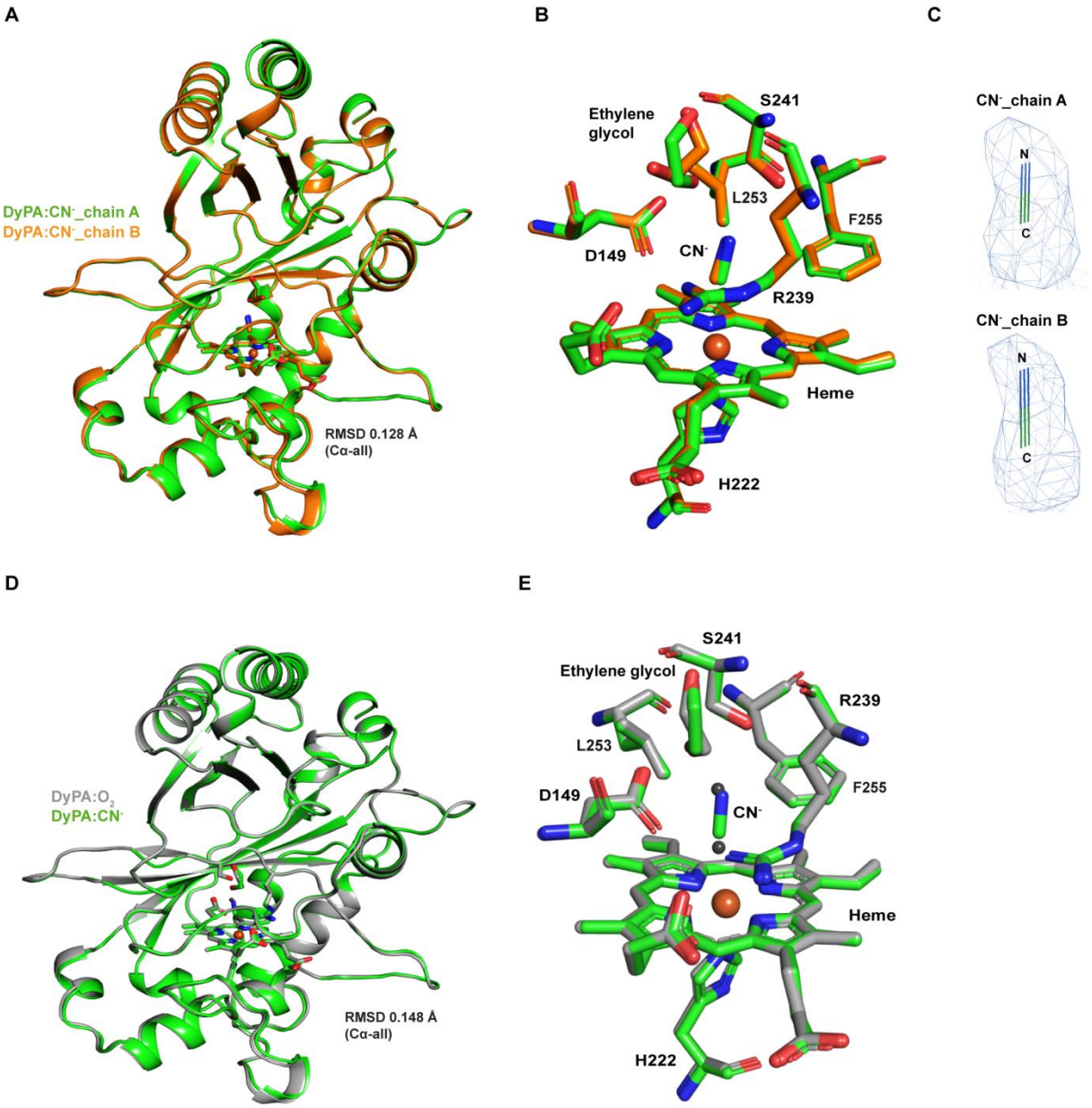


**Figure S7:** Structure of *Dictyostelium* DyPA:$CN^-$ complex. **(A)** Structural alignment of both copies of the *Dictyostelium* DyPA:$CN^-$ complex in the asymmetric unit reveals that both copies are nearly identical. **(B)** Heme microenvironment of the *Dictyostelium* DyPA:$CN^-$. (**C)** OMIT electron density maps of $CN^-$ moieties, contoured at 1.5σ. **(D)** Structural alignment of single monomers for the *Dictyostelium* DyPA:$O_2$ complex structure (grey) and *Dictyostelium* DyPA:$CN^-$ complex (green). **(E)** Overlay of the heme microenvironment of the *Dictyostelium* DyPA $CN^-$ (green) and activated $O_2$ (grey) complexes. The atoms of the activated oxygen molecule are shown as grey spheres and iron atom of the heme is shown as a red sphere, in the *Dictyostelium* DyPA:$O_2$ complex structure.

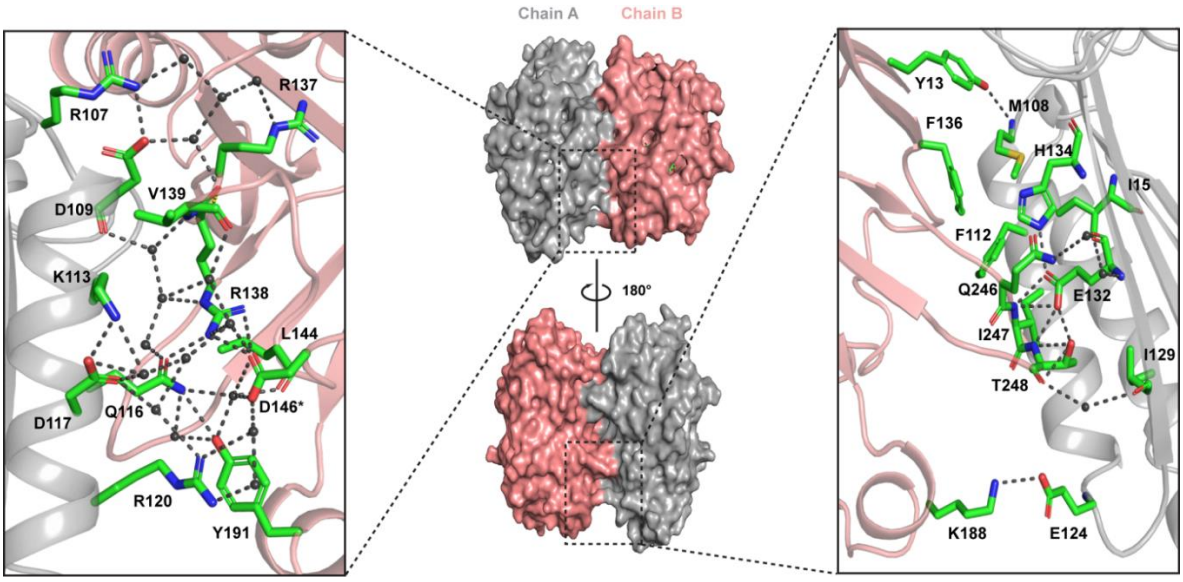


**Figure S8:** *Dictyostelium* DyPA:$O_2$ complex dimer interface. The individual *Dictyostelium* DyPA monomers are shown in grey and salmon pink. Surface and cartoon representations of *Dictyostelium* DyPA dimer. Selected amino acids are colored in the atomic color scheme. Water molecules are shown as grey spheres. Key non-covalent bonds are represented as grey dashed lines; the bond length cutoff is 3.5 Å.

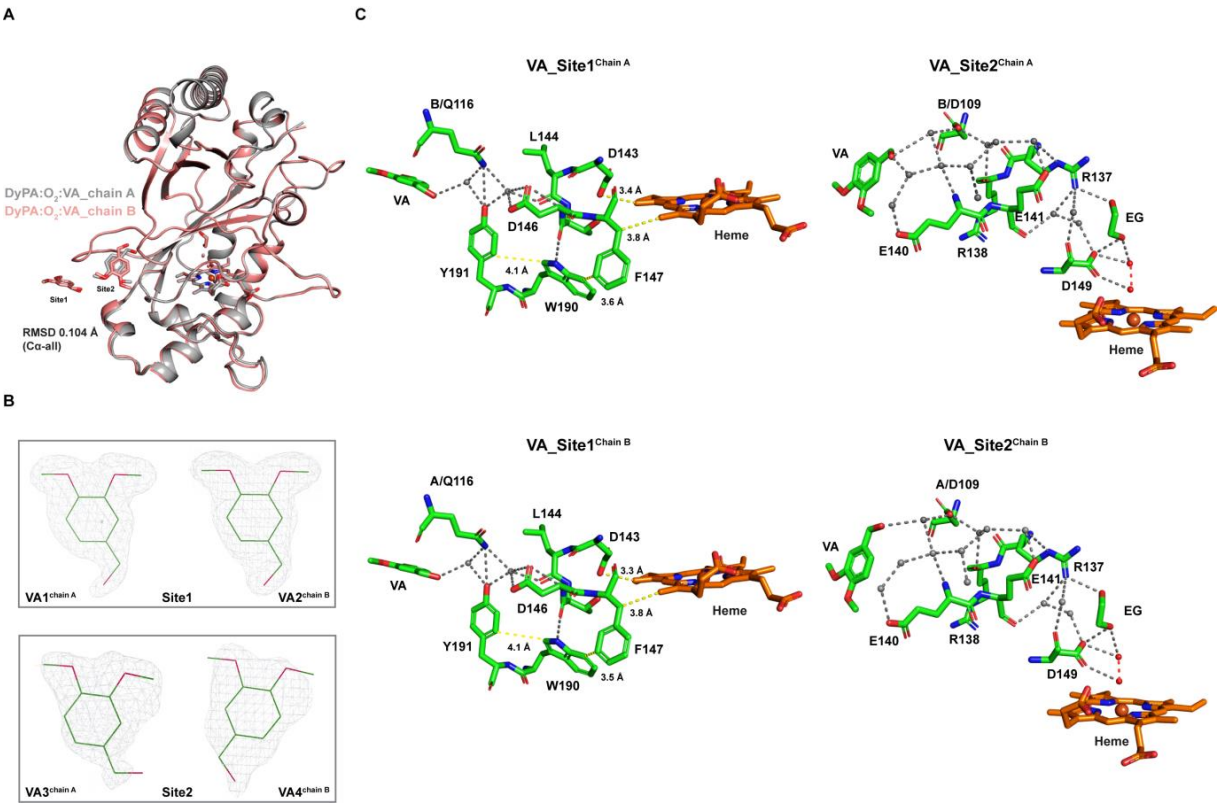


**Figure S9:** Structure of the *Dictyostelium* DyPA:O2:VA complex. **(A)** Structure of *Dictyostelium* DyPA:O2:VA complex. (A) Structural alignment of both copies of the *Dictyostelium* DyPA:O2:VA complex in the asymmetric unit reveals that both copies are nearly identical (C$\alpha$-RMSD of 0.105 Å). **(B)** OMIT electron density maps for bound VA molecules, contoured at 1$\sigma$. **(C)** Proposed long-range electron transfer pathways from veratryl alcohol binding sites to the heme moiety of *Dictyostelium* DyPA. The atoms of the activated oxygen molecules are shown as red spheres and the water molecules are shown as grey spheres. Hydrogen bonds are represented as grey dashed lines.

**Table S1.** Data-collection and refinement statistics
(values in parentheses are for the outer shell).

| | **DyPA:$O_2$** | **DyPA:$CN^-$** | **DyPA:$O_2$:VA** |
|---|---|---|---|
| **Data collection**[#] | | | |
| X-Ray Source | ID29, ESRF Grenoble | ID29, ESRF Grenoble | ID23-1, ESRF Grenoble |
| Wavelength (Å) | 0.91985 | 0.91985 | 0.910003 |
| Crystal-to-detector distance (mm) | 313.233 | 288.91 | 318 |
| Exposure time per image (s) | 0.0375 | 0.0375 | 0.0375 |
| No. of images | 1200 | 1200 | 3000 |
| Oscillation range (°) | 0.3 | 0.3 | 0.15 |
| Resolution range (Å) | 47.78-1.7(1.79-1.7) | 47.74-1.85 (1.94-1.85) | 47.64-1.60 (1.63-1.60) |
| Space group | $P4_12_12$ | $P4_12_12$ | $P4_12_12$ |
| Unit cell<br>a,b,c (Å)<br>$\alpha, \beta, \gamma$ (°) | <br>141.03, 141.03, 95.56<br>90, 90, 90 | <br>141.05, 141.05, 95.48<br>90, 90, 90 | <br>140.44, 140.44, 95.28<br>90, 90, 90 |
| Crystal mosaicity (°) | 0.13 | 0.115 | 0.097 |
| No. of molecules in AU | 2 | 2 | 2 |
| Wilson B-factor | 23.4 | 25.8 | 21.1 |
| Total reflections | 2811648 | 2170478 | 4163950 |
| Unique reflections | 105810 | 82374 | 125165 |
| Multiplicity | 26.6 (25.4) | 26.4 (26.2) | 33.26 (33.48) |
| Completeness (%) | 100 (100) | 100 (100) | 100 (100) |
| Mean I/sigma(I) | 18.5 (2.9) | 15.4 (2.9) | 25.13 (3.7) |
| $R_{sigma}$ (%) | 3.1 (36.1) | 3.9 (36.2) | 2.3 ( 27.9) |
| $R_{int}$ (%) | 13.67 (77) | 15.14 (81) | 10.38 (74) |
| **Refinement** | | | |
| Resolution range (Å) | 45.25-1.7 | 45.22-1.85 | 45.11-1.60 |
| Reflections used in refinement | 105721 | 82292 | 125077 |
| Reflections used for R-free | 5281 | 4123 | 6292 |
| $R_{work}$ (%) | 14.71 | 15.59 | 15.2 |
| $R_{free}$ (%) | 16.5 | 17.99 | 16.8 |
| **Stereochemical parameters** | | | |
| Number of non-hydrogen atoms<br>Macromolecules<br>Ligands<br>Water | 5647<br>613<br>9<br>618 | 5429<br>612<br>11<br>393 | 5729<br>614<br>10<br>618 |
| R.m.s deviations<br>Bond length (Å)<br>Bond angles (°) | <br>0.007<br>1.098 | <br>0.007<br>1.103 | <br>0.006<br>1.161 |
| Ramachandran plot<br>Favored (%)<br>Additionally allowed (%)<br>Outliers (%) | <br>99.18<br>0.82<br>0 | <br>99.51<br>0.49<br>0 | <br>99.18<br>0.82<br>0 |
| B-factors (Å$^2$) | 30.00 | 33.00 | 29.00 |
| PDB ID | 7O9J | 7O9L | 7ODZ |

# $R_{free}$ is calculated for a randomly chosen 5 % subset of reflections.